are not modeled. Thus, there is a strong need for adequate modeling.

Conclusions

The technical feasibility of using a strapdown stellar sensor for inflight platform error calibration has been demonstrated. The conceptual method permits a shift of the system accuracy-maintenance burden from pre-flight calibration to in-flight computation. The sample case, although limited in general applicability, demonstrates the potential effectiveness of the concept presented.

References

[1] Nash, J. M., "On the Use of a Simple Stellar Sighter to Determine Booster Navigation Error Parameters," Ph.D. thesis, March 1974, Engineering Systems Department, University of California, Los Angeles, Calif.

[2] Meditch, J. S., *Stochastic Optimal Linear Estimation and Control*, McGraw-Hill, New York, 1969.

[3] Birnbaum, M. M. and Salomon, P. M., "Strapdown Star Tracker for Space Vehicle Attitude Control," *Journal of Spacecraft and Rockets*, Vol. 5, Oct. 1968, pp. 1188–1192.

[4] Goldstein, H., *Classical Mechanics*, Addison-Wesley, Reading, Mass., 1950.

MAY 1975 AIAA JOURNAL VOL. 13, NO. 5

Buckling and Vibration of Cross-Ply Laminated Circular Cylindrical Shells

ROBERT M. JONES* AND HAROLD S. MORGAN†
SMU Institute of Technology, Dallas, Texas

Numerical results from an exact solution are presented for buckling and vibration of simply supported circular cylindrical shells that are laminated unsymmetrically about their middle surface. The coupling between bending and extension induced by the lamination asymmetry substantially decreases buckling loads and vibration frequencies for common composite materials such as boron/epoxy and graphite/epoxy. For antisymmetric laminates, the effect of the coupling dies out rapidly as the number of layers is increased. However, for generally unsymmetric laminates, the effect of coupling dies out very slowly as the number of layers is increased. That is, having a large number of layers is no guarantee that coupling will not seriously degrade the shell buckling resistance and vibration frequencies. Thus, coupling between bending and extension must be included in all analyses of unsymmetrically laminated shells.

Nomenclature

A_{ij}, B_{ij}, D_{ij} = extensional, coupling, and bending stiffnesses of a laminated shell
E_1 = Young's modulus in the 1-direction of a lamina
E_2 = Young's modulus in the 2-direction of a lamina
G_{12} = shearing modulus in the 1–2 plane of a lamina
k_x = normalized axial compression, Eq. (7)
k_y = normalized lateral pressure, Eq. (13)
k_ω = normalized vibration frequency, Eq. (15)
L = shell length (Fig. 1)
m = number of buckle or vibration halfwaves in the x-direction
NL = number of layers in a laminated shell
$\bar{N}_x, \bar{N}_y$ = applied in-surface forces in the x- and y-directions, respectively
n = number of buckle or vibration halfwaves in the y-direction
r = shell radius to the middle surface (Fig. 1)
t = total laminate thickness (Fig. 1)
Z = modified Batdorf shell curvature parameter, Eq. (9)
x, y, z = shell coordinates (Fig. 1)
ν_{12} = Poisson's ratio for contraction (expansion) in the 2-direction due to tension (compression) in the 1-direction

Presented as Paper 74-33 at the 12th AIAA Aerospace Sciences Meeting, Washington, D. C., January 30–February 1, 1974; submitted January 30, 1974; revision received September 20, 1974. This work was partially supported by the Air Force Office of Scientific Research/NA, Air Force Systems Command, USAF, under AFOSR Grant 73-2532.

Index categories: Structural Composite Materials (Including Coatings); Structural Stability Analysis; Structural Dynamic Analysis.

* Associate Professor of Solid Mechanics. Associate Fellow AIAA.
† Research Assistant.

Introduction

CROSS-PLY laminated circular cylindrical shells as in Fig. 1 are common structural elements in the aerospace industry. The advent of advanced fiber-reinforced composite materials such as boron/epoxy and graphite/epoxy with their high potential weight savings has resulted in a significant increase in the use of cross-ply laminated fiber-reinforced shells. Therefore, general knowledge of their vibration frequencies and resistance to buckling is essential. Furthermore, knowledge of their behavior sheds light on the behavior of more complicated laminates such as angle-plys and laminates with mixed orientations.

An important step in learning how to properly laminate shells is to understand the influence of lamination asymmetries about the shell middle surface. Those asymmetries cause coupling

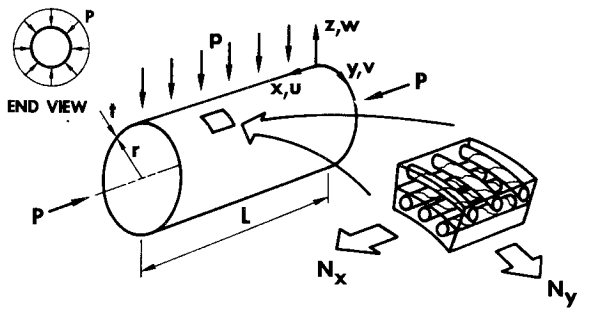

Fig. 1 Laminated shell geometry and loading.

between bending and extension of the laminate. This phenomenon is evidenced by *bending* of a laminate that is subjected to only in-plane or in-surface forces or *extension* of a laminate that is bent by the application of moments alone. Another example is bending of a laminate that is subjected to a uniform temperature rise; this is the principle by which the common thermostat works. For unsymmetrically laminated plates, the coupling results in significantly decreased buckling loads and vibration frequencies.[1] Bending effects for symmetrically laminated plates are uncoupled from extensional effects. In contrast, for symmetrically laminated shells, bending effects are always coupled to extensional effects. However, that coupling is quite small if the shell is flat enough (nearly a plate). For unsymmetrically laminated shells, buckling loads and vibration frequencies are reduced, but normalized results and general conclusions in the manner of Whitney and Leissa's plates results[1] do not exist to the authors' knowledge.

The objective of this paper is to present extensive numerical results for buckling and vibration of laminated circular cylindrical shells as depicted in Fig. 1. Attention is restricted to cross-ply laminates, i.e., laminates with laminae (plys) that have their principal material directions (one being the fiber direction) aligned with the axial and circumferential coordinates of the shell. That is, the fibers in one layer are in the axial direction whereas, in the next layer, the fibers are in the circumferential direction. In the theory, any sequence of 0° (axial) and 90° (circumferential) layers can be considered.

Further description of the differences between the various classifications of cross-ply laminates is appropriate because of the similarity of the phrases used to designate each class. First of all, the adjective regular is suggested by the writers to describe laminates with equal thickness laminae as in the top half of Fig. 2. Irregular or nonregular laminates have laminae of arbitrary, different thicknesses. Hereafter, dropping the adjective "regular" implies that the laminae are of unequal thickness, i.e., the term "irregular" will not be explicitly used, but is the default adjective. Also shown in Fig. 2 are examples of symmetric, antisymmetric, and unsymmetric laminates. Symmetric laminates have both geometric and material property symmetry about the middle surface. Antisymmetric laminates have geometric symmetry and material property antisymmetry. Unsymmetric laminates could have geometric symmetry, but do not have material property symmetry or antisymmetry.

The behavior of laminates that are symmetric, antisymmetric, or unsymmetric about the shell middle surface is studied in the present paper. Symmetric laminates can be treated with conventional orthotropic shell theory. Antisymmetric laminates have a simple form of coupling between bending and extension and therefore require a more complicated theory than symmetric laminates. Unsymmetric laminates have more complicated coupling between bending and extension than do antisymmetric laminates. The governing theory for buckling of these laminates is due to Jones[2] and involves Donnell-type shell theory. Dong[3] derived a similar theory for vibration problems. Exact solutions were obtained for S2 simply supported edge boundary conditions as defined by Almroth.[4] These theories are much simpler (although admittedly somewhat less accurate) than that of Cheng and Ho.[5]

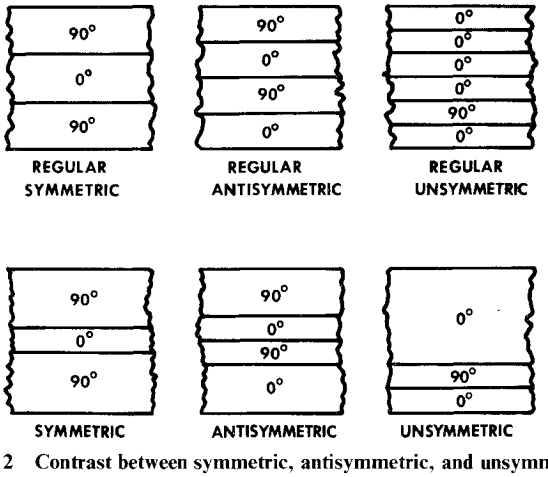

Fig. 2 Contrast between symmetric, antisymmetric, and unsymmetric cross-ply laminates.

Representative results are given for each class of laminated shells. For symmetric and antisymmetric laminates, the results are normalized relative to pertinent shell parameters to provide a better basis for understanding the behavior of a wide class of shell buckling and vibration problems. These general results are much more comprehensive than the results heretofore available for specific shells. For unsymmetric laminates, the generality of lamination dictates that general numerical results cannot be obtained. Therefore, a special unsymmetric laminate is studied numerically. Pertinent parameters of the numerical results include material properties, length-to-radius ratio, and radius-to-thickness ratio.

Specifically, we seek to confirm the expectation that the effect of coupling between bending and extension on buckling loads and vibration frequencies dies out rapidly as the number of layers increases for antisymmetric laminates. Also, for the special unsymmetric laminate, we expect to find that the effect of coupling dies out quite slowly as the number of layers increases in analogy to similar work on unsymmetrically laminated plates by Jones.[6]

Buckling and Vibration Criterion

The Donnell-type differential equations governing buckling and vibrations of laminated shells are commonly expressed in terms of variations of in-surface forces and moments which can be subsequently expressed in terms of variations of displacements during buckling or vibration. The solution to the governing differential equations for unsymmetrically laminated cross-ply shells with S2 simply supported edge boundary conditions is straightforward. The result is a simple closed form buckling and vibration criterion that is applicable for various combinations of in-surface forces $\bar{N}_x$ and $\bar{N}_y$ due to axial compression and lateral pressure, respectively:

$$\rho\omega^2 - \bar{N}_x(m\pi/L)^2 - \bar{N}_y(n/r)^2 = T_{33} + (2T_{12}T_{13}T_{23} - T_{11}T_{23}^2 - T_{22}T_{13}^2)/(T_{11}T_{22} - T_{12}^2) \quad (1)$$

in which

$$\begin{aligned}
T_{11} &= A_{11}(m\pi/L)^2 + A_{66}(n/r)^2 \\
T_{12} &= (A_{12} + A_{66})(m\pi/L)(n/r) \\
T_{13} &= (A_{12}/r)(m\pi/L) + (B_{12} + 2B_{66})(m\pi/L)(n/r)^2 + B_{11}(m\pi/L)^3 \\
T_{22} &= A_{22}(n/r)^2 + A_{66}(m\pi/L)^2 \\
T_{23} &= (A_{22}/r)(n/r) + (B_{12} + 2B_{66})(m\pi/L)^2(n/r) + B_{22}(n/r)^3 \\
T_{33} &= D_{11}(m\pi/L)^4 + 2(D_{12} + 2D_{66})(m\pi/L)^2(n/r)^2 + \\
&\quad D_{22}(n/r)^4 + (2B_{22}/r)(n/r)^2 + A_{22}/r^2 + (2/r)B_{12}(m\pi/L)^2
\end{aligned} \quad (2)$$

where the A_{ij}, B_{ij}, and D_{ij} are the usual cross-ply laminate extensional, coupling, and bending stiffnesses defined in terms of the lamina principal material properties E_1, E_2, ν_{12}, and G_{12} by, e.g., Jones.[7] Note that the stiffnesses A_{16}, A_{26}, B_{16}, B_{26}, D_{16}, and D_{26} are zero for cross-ply laminates.

The buckling and vibration criterion in Eq. (1) is the exact solution to the title problem when prebuckling deformations and tangential inertia terms are ignored. Jones[2] obtained the buckling criterion which results when vibrations are ignored. Dong[3] obtained a vibration solution which reduces to Eq. (1) when his tangential inertia terms are ignored. A complete derivation of the buckling and vibration criterion in Eq. (1) in conventional nomenclature for laminated composites is given by Jones and Morgan.[8]

For buckling problems, the buckling loads result when $\omega = 0$ in Eq. (1). As an example, for $\bar{N}_x$ only,

$$\bar{N}_x = -[L/(m\pi)]^2 \mathrm{RHS} \quad (3)$$

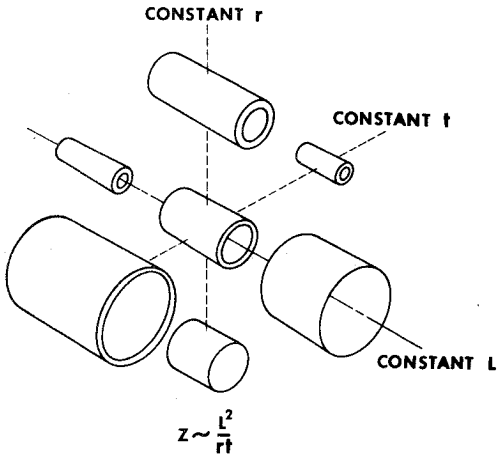

Fig. 3 Representative circular cylindrical shells having the same value of the Batdorf curvature parameter Z (Z about 150).

where RHS is the right-hand side of Eq. (1). Or for combinations of $\bar{N}_x$ and $\bar{N}_y$,

$$\bar{N}_x = -\text{RHS}/[(m\pi/L)^2 + k(n/r)^2] \tag{4}$$

wherein $\bar{N}_y = k\bar{N}_x$ (k is a specified constant). In all cases, the lowest buckling load must be found by minimizing the right-hand side of an equation like Eqs. (3) or (4) for integer values of m and n which determine the buckle mode shape.[9] Because of the numerous parameters involved and the many repetitive calculations in the minimization procedure, a computer program (BOLS II for Buckling of Laminated Shells, Version II) was written; numerical results are discussed in the next two sections.

For free vibration problems without prestress, the natural frequencies are

$$\omega = (\text{RHS}/\rho)^{1/2} \tag{5}$$

where the associated mode shapes are the variations in displacements with the mode numbers m and n substituted corresponding to the values used in RHS to determine ω. The fundamental natural frequency is the lowest ω and is obtained by the minimization procedure involving integer values of m and n.[9] The vibration results of the program for isotropic shells were verified by comparison with tabulated results in the excellent monograph by Leissa.[10]

For free vibration problems with prestress, the vibration frequencies are

$$\omega = \{[\text{RHS} + \bar{N}_x(m\pi/L)^2 + \bar{N}_y(n/r)^2]/\rho\}^{1/2} \tag{6}$$

with mode shapes and fundamental natural frequency found as for free vibrations.

Antisymmetric Laminate Results

Basic normalized design analysis results are presented for buckling and vibration of antisymmetrically laminated cross-ply circular cylindrical shells. In both cases, the familiar Batdorf k-Z normalization is attained after Eq. (1) is specialized for antisymmetric cross-ply laminates ($A_{11} = A_{22}$, $B_{11} = -B_{22}$, $B_{12} = B_{66} = 0$, and $D_{11} = D_{22}$).

Axial Compression Buckling Results

For axial compression, Eq. (1) can be rearranged as

$$\begin{aligned} k_x = -\bar{N}_x L^2/\pi^2 D_{11} = m^2\{1 + 4[D_{66}/D_{11} + \\ \nu_{12}F/(1+F)](nL/m\pi r)^2 + (nL/m\pi r)^4\} + 12Z^2/(m^2\pi^4 A) - \\ (B_{11}^2/A_{11}D_{11})\{1 + (A_{11}/A_{66})(nL/m\pi r)^2 + \\ 2[2\nu_{12}F/(1+F) + 1](nL/m\pi r)^4 + (A_{11}/A_{66})(nL/m\pi r)^6 + \\ (nL/m\pi r)^8\}(m^2/A) + 4(L^2/r)(B_{11}/D_{11})[\nu_{12}F/(1+F)] \times \\ [(nL/m\pi r)^4 + 1]/(\pi^2 A) \end{aligned} \tag{7}$$

where

$$F = E_2/E_1 \tag{8}$$

$$Z = (L^2/rt)[1 - 4\nu_{12}^2F^2/(1+F)^2]^{1/2} \tag{9}$$

$$\begin{aligned} A = 1 + \{(A_{11}/A_{66})[1 - 4\nu_{12}^2F^2/(1+F)^2] - \\ 4\nu_{12}F/(1+F)\}(nL/m\pi r)^2 + (nL/m\pi r)^4 \end{aligned} \tag{10}$$

For isotropic materials, the function Z in Eq. (9) is the well-known Batdorf shell curvature parameter. For constant material properties, the physical interpretation of Z is related to the geometric expression L^2/rt. Thus, the single parameter Z can be used to represent many different shells, i.e., many different combinations of L, r, and t as in Fig. 3.

The expression for k_x, Eq. (7) has four terms: 1) an orthotropic plate bending contribution; 2) a shell curvature component; 3) a contribution of lamination effects; and 4) coupling between lamination effects and curvature effects. Terms 1) and 2) are found in classical shell theory. Terms 1) and 3) are found in classical laminated plate theory. Thus, the fourth term has a new parameter that has not been discussed before.

The coefficient on the lamination effects term can be shown to be

$$B_{11}^2/A_{11}D_{11} = 3(F-1)^2/[(NL)^2(1+F)^2] \tag{11}$$

where NL is the number of layers in the laminate. Thus, as the number of layers increases, the lamination effects term decreases rapidly. The rapid decrease of this term is responsible for the rapid approach of laminated plate buckling loads to orthotropic plate results as determined by Whitney and Leissa.[1]

The coefficient on the lamination/curvature coupling effects term reduces to

$$(L^2/r)(B_{11}/D_{11}) = 6(L^2/rt)(F-1)/[(NL)(1+F)] \tag{12}$$

This coefficient approaches zero only as the inverse of NL as opposed to the inverse of $(NL)^2$ for the lamination effects coefficient. Note that the component L^2/rt is the Batdorf shell curvature parameter with all association with material properties removed.

Axial compression k_x–Z results for antisymmetrically laminated graphite/epoxy shells are shown in Fig. 4 for 2, 4, and an infinite number of layers. The results for an infinite number of layers are the same as the orthotropic solution in which all coupling between bending and extension is ignored (then, B_{11}, the only coupling stiffness for an antisymmetric cross-ply

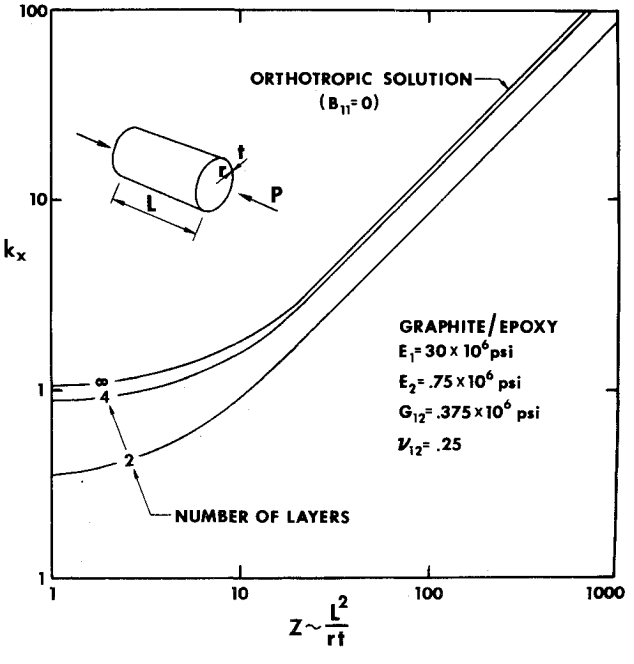

Fig. 4 Normalized axial compression buckling loads of antisymmetric cross-ply laminated graphite/epoxy shells.

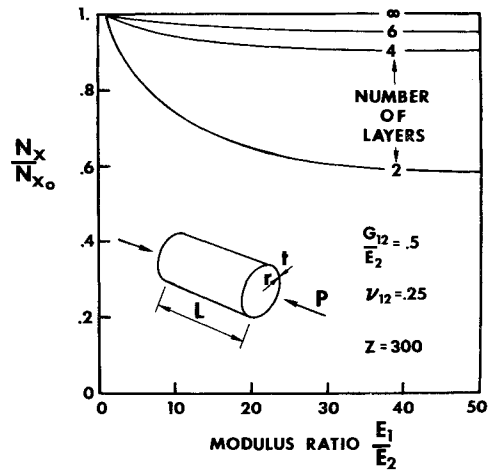

Fig. 5 Relative axial compression buckling loads of antisymmetric cross-ply laminated shells.

laminate, is zero). Because of the log-log plot, the large percentage differences between the buckling loads for laminates with different numbers of layers are obscured. The well-known large coupling effects for plates are detected by observing that all curves are far apart for $Z = 1$. For $Z > 20$, $k_x - Z$ results for various numbers of layers have the same slope so have a constant relation to one another. However, the effect of coupling between bending and extension is less for a long shell ($Z > 20$) than for a plate. The orthotropic approximation ($B_{11} = 0$) is too high at $Z = 100$ by 67% for two-layered shells and by 9% for four-layered shells. For more than 4 layers, the coupling effect is negligible. Thus, the effect of coupling between bending and extension rapidly dies out as the number of layers increases.

For other composite materials, when the shell length, radius, and thickness are fixed, the buckling loads depend essentially on the modulus ratio, E_1/E_2. The buckling loads when $Z = 300$ are plotted as a function of E_1/E_2 in Fig. 5 relative to the buckling load of an orthotropic shell ($B_{11} = 0$). Values of G_{12}/E_2 and ν_{12} are fixed because their influence on the buckling load is small compared to E_1/E_2. The curves plotted are actually envelopes to the curves with cusps (due to buckle mode shape changes) that exist for a specific shell geometry. For other L, r, and t for $Z = 300$, the curves vary so as to fit above the envelopes plotted. At any rate, the specific numerical values are not as important as the general influence of the modulus ratio.

The relative buckling loads decrease with increasing E_1/E_2. For a boron/epoxy shell ($E_1/E_2 = 10$), the effect of coupling is not quite as striking as for the graphite/epoxy ($E_1/E_2 = 40$) shells already discussed. However, the effect of coupling is still substantial for low numbers of layers.

Lateral Pressure Buckling Results

For lateral pressure, Eq. (1) can be written as

$$k_y = -\bar{N}_y L^2/\pi^2 D_{11} = (m\pi r/nL)^2 k_x \tag{13}$$

and thus has the same components (orthotropic plate bending, etc.) as the normalized axial compression buckling load. For long shells, $nL/m\pi r$ is much greater than one so Eq. (13) has minimum value

$$k_y = CZ^{1/2} \tag{14}$$

where C is a function of the lamination properties including the number of layers. For isotropic shells, $C = (4/3)3^{1/2}$. For 2 layers, the value of C is less than for 4 layers which in turn is less than for 6 layers and so on. Thus, the $k_y - Z$ results for long graphite/epoxy shells in Fig. 6 are not parallel but instead diverge for large values of Z. That is, the effect of coupling between bending and extension increases with increasing Z. For example, the orthotropic approximation to the two-layered shell buckling load is about 120% too high at $Z = 100$ and about 140% too high at $Z = 10{,}000$. Generally, however, the effect of coupling dies out rapidly with an increasing number of layers for all shells.

The lateral pressure buckling loads normalized relative to orthotropic shell buckling loads are plotted for various modulus ratios, E_1/E_2, in Fig. 7. Again, E_1/E_2 is used to display the essence of the behavior of various composite materials whereas G_{12}/E_2 and ν_{12} are fixed because their effect is less important. As for axial compression, only the envelopes of the actual curves are plotted. The effect of coupling for a two-layered shell is much greater than for axial compression. Even for a boron/epoxy shell ($E_1/E_2 = 10$), the actual buckling load is only 60% of the predicted value for orthotropic shells (where coupling is ignored). That is, the orthotropic approximation is too high by 67% for boron/epoxy shells and by 127% for graphite/epoxy shells. These overestimates of buckling resistance die out rapidly as the number of layers increases.

Vibration Results

For vibration, Eq. (1) can be written as

$$k_\omega = (\omega L^2/\pi^2)(\rho/D_{11})^{1/2} = m^2 k_x^{1/2} \tag{15}$$

and has the same basic components (orthotropic plate bending, etc.) as the normalized axial compression and lateral pressure

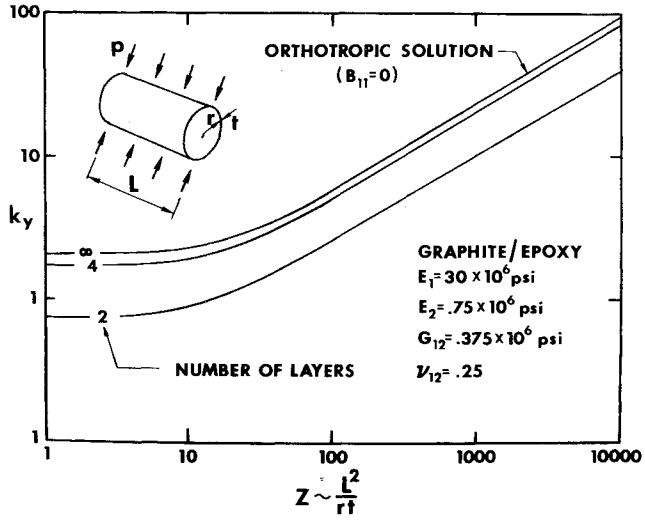

Fig. 6 Normalized lateral pressure buckling loads of antisymmetric cross-ply laminated graphite/epoxy shells.

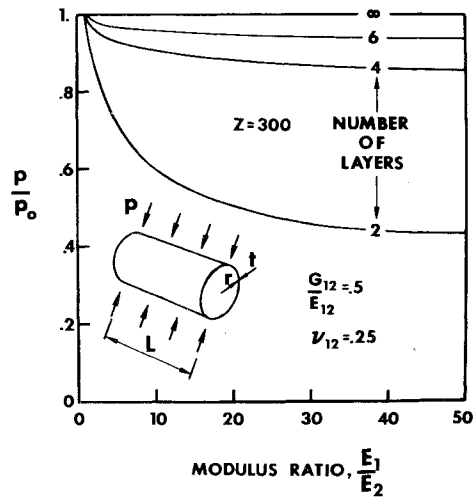

Fig. 7 Relative lateral pressure buckling loads of antisymmetric cross-ply laminated shells.

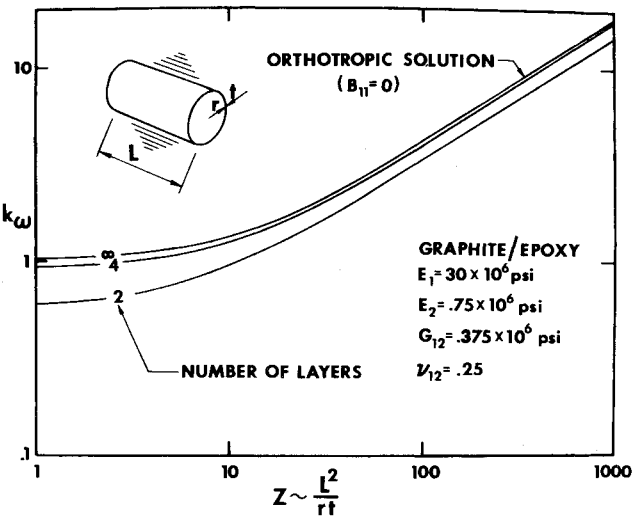

Fig. 8 Normalized fundamental natural frequencies of antisymmetric cross-ply laminated graphite/epoxy shells.

buckling loads. Equation (15) reduces for isotropic shells to the results of Mikulas and McElman.[11] The normalized fundamental natural frequency for graphite/epoxy shells is plotted vs the modified Batdorf curvature parameter in Fig. 8. The effect of coupling between bending and extension on vibration frequencies is not nearly as high as on axial compression and lateral pressure buckling loads. The principal reason for this result is that vibration frequencies are related to the square root of the same function from which the buckling loads are obtained. Thus, differences between curves for various numbers of layers are diminished substantially. Those differences are essentially constant with Z as for axial compression, but unlike lateral pressure.

The fundamental natural frequencies for various modulus ratios, E_1/E_2, are plotted in Fig. 9 after being normalized relative to the frequencies for an orthotropic shell. Of course, only the envelopes of results for $Z = 300$ are presented. Obviously, the effects of coupling do not increase much after E_1/E_2 reaches 10 (a typical value for boron/epoxy). That is, boron/epoxy $k_\omega - Z$ results are very close to the graphite/epoxy results in Fig. 8.

Summary

For both buckling and vibration of antisymmetrically laminated cross-ply shells, the effect of coupling between bending and extension dies out rapidly as the number of layers increases. For shells under lateral pressure, the effect of coupling is larger for long shells than for moderate length shells. For axial compression and vibration of long shells, the effect of coupling is essentially constant with increasing Z, the modified Batdorf curvature parameter.

For both buckling and vibration problems, switching the layer stacking sequence from 0°/90°/... to 90°/0°/... does not change the buckling loads or vibration frequencies. For a two-layered shell, a large difference might be expected when an analogy is made with the stiffener eccentricity effect[12] which is another form of bending-extension coupling. Both the lamination effect and the stiffener eccentricity effect have terms which 1) change sign depending on either lamination sequence or stiffener placement (on the outside or the inside of the shell) and 2) occupy the same positions in the governing buckling differential equation and solution[2]. For an axially compressed circular cylindrical shell with longitudinal stiffeners (stringers), the buckling load for externally placed stringers can be twice or three times the buckling load for internal stringers. For the same loading, higher buckling loads are obtained for shells with internal rings than for shells with external rings. The buckling loads and vibration frequencies for 0°/90°/... shells are the same as for 90°/0°/... shells because a laminated shell is actually analogous to a shell with simultaneous ring and stringer stiffening (same stiffener sizes and spacings) on the same side of the shell. That is, a laminate is inherently a two-dimensional element whereas a stiffener is idealized as a one-dimensional element. Thus, a laminate has effects which are mutually counteracting.

Table 1 Buckling and vibration results for antisymmetric cross-ply laminated graphite/epoxy cylindrical shells ($r = 10.0, t = 0.10, E_1 = 30 \times 10^6$ psi, $E_2 = 0.75 \times 10^6$ psi, $G_{12} = 3.75 \times 10^6$ psi, $\nu_{12} = 0.25$)

L	Z	Number of layers	k_x	k_y	k_ω
		2	0.35636	0.73758	0.59696
1.00	1	4	0.87041	1.7685	0.93296
		∞	1.0408	2.1121	1.0202
		2	0.90101	0.89741	0.94921
3.16	10	4	1.5857	1.9656	1.2593
		∞	1.7982	2.3164	1.3410
		2	8.7406	2.6910	3.3874
10.00	100	4	13.310	5.1606	4.0103
		∞	14.567	5.8367	4.1673
		2	86.153	10.788	14.280
31.63	1000	4	132.84	20.930	17.580
		∞	145.37	23.750	17.998

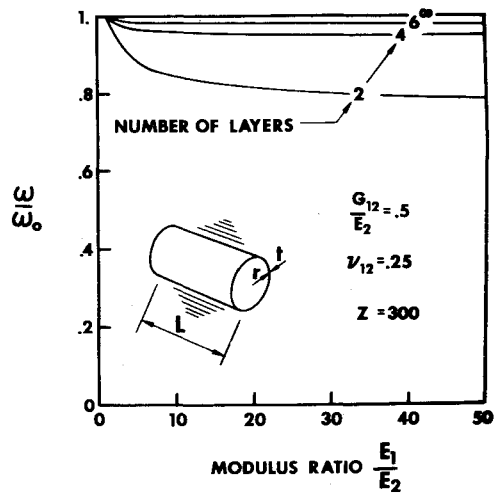

Fig. 9 Relative fundamental natural frequencies of antisymmetric cross-ply laminated shells.

Specific numerical results for buckling and vibration corresponding to selected values in Figs. 4, 6, and 8 are given in Table 1 to provide a better basis for comparison with other numerical results than scaling curves. More significant figures than practically necessary are shown for ease of checking computer results (these results were obtained on a CDC CYBER-72).

Unsymmetric Laminate Results

Because of the infinite complexity of the class of unsymmetric laminates, general results are impossible. Instead, the specific, but representative unsymmetric laminate example in Fig. 10 is considered. There, the fibers in the second layer from the bottom are oriented at 90° and the fibers in all other layers are oriented at 0° to the shell x-axis. That is, the laminate has predominantly layers with axial fibers, but one layer has circumferential fibers. Thus, as the number of layers increases for a constant thickness laminate, the 90° layer gets thinner and moves toward the bottom of the laminate. This example is contrived (i.e., probably not ever encountered in engineering practice), but is a simple, straight-forward example of unsymmetric

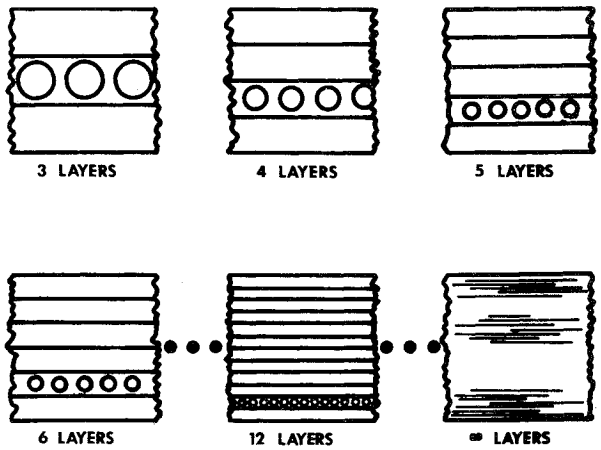

Fig. 10 Unsymmetric laminate example.

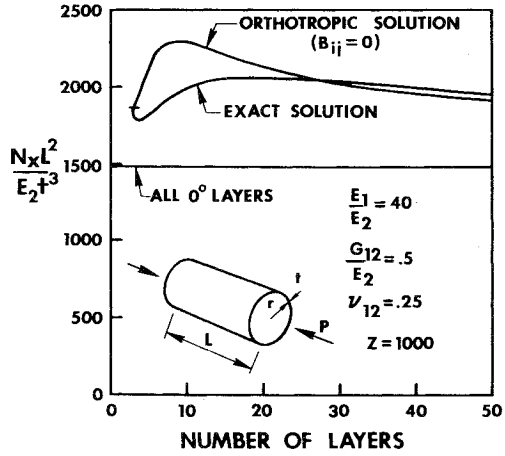

Fig. 11 Normalized axial compression buckling loads of unsymmetric cross-ply laminated graphite/epoxy shells.

laminates that is amenable to rather comprehensive theoretical parametric study with the objective of understanding unsymmetric laminates.

Axial Compression Buckling Results

Normalized axial compression buckling loads for an unsymmetrically laminated graphite/epoxy shell are shown in Fig. 11 as a function of the number of layers. The shell has all 0° layers except for one 90° layer and a length, radius, and thickness such that $Z = 1000$. One of the baseline comparison values is the buckling load for a shell with all 0° layers. The other comparison case is an unsymmetrically laminated shell for which coupling between bending and extension is ignored ($B_{ij} = 0$). Results for the actual unsymmetrically laminated shell, for which coupling between bending and extension is considered, are labeled exact solution in Fig. 11.

The actual laminate has, not surprisingly, less buckling resistance than a laminate with $B_{ij} = 0$ except when the laminate has a large number of layers. On the other hand, the actual laminate has more buckling resistance than a laminate with all 0° layers. The reason for this curious result is related to the relative values of the stiffnesses in the x- and y- directions and as well to the shell parameters. As will be seen subsequently, D_{11} is decreased somewhat by the presence of a 90° layer, but D_{22} is most easily examined for a three-layered shell which is, of course, symmetric. Thus, the exact solution corresponds to the orthotropic solution ($B_{ij} = 0$), e.g., see the horizontal hash mark at three layers in Fig. 11 where the two curves coincide. At that point, the solution for an orthotropic plate which buckles into the $m = 1$, $n = 1$ mode is

$$N_x L^2 = \pi^2[D_{11}/4 + 2(D_{12} + 2D_{66}) + 4D_{22}] \qquad (16)$$

which is readily obtained from Eq. (1). For a graphite/epoxy laminate, the term in Eq. (16) involving D_{11} decreases by less than 4% when the actual laminate is considered as opposed to the all 0° layer laminate. On the other hand, the term involving D_{22} is $2\frac{1}{2}$ times as big for the actual laminate as it is for the all 0° layer laminate. The net result is 33% bigger for the actual laminate than for the all 0° layer laminate.

The differences between the exact and orthotropic predictions for graphite/epoxy laminates in Fig. 11 range from 18% less than the orthotropic solution ($B_{ij} = 0$) at 6 layers to 12% less at 10 layers to 2% more at 50 layers. In addition, the exact results range from about 38% more than the all 0° laminate results at 20 layers to about 30% more at 50 layers. Such differences are well within the consideration of usual engineering design practice. However, the differences exist for many more layers than coupling between bending and extension was believed to be important. That belief was established on the basis of extrapolating antisymmetric cross-ply results. Obviously, such extrapolation is invalid.

As an aid to understanding the buckling behavior illustrated in Fig. 11, the extensional, coupling, and bending stiffnesses are plotted vs the number of layers in Fig. 12 for graphite/epoxy. The stiffnesses in the x-direction (with which most fibers are aligned), A_{11} and D_{11}, are nearly independent of the number of layers. However, the 90° layer causes the stiffnesses in the y-direction, A_{22} and D_{22}, to deviate by up to an order of magnitude from the value for all 0° layers (which is the same as the value for an infinite number of layers). These discrepancies die out very slowly as the number of layers increases. Moreover, the normalized stiffness for coupling between bending and extension, which can be shown to be

$$B_{11}/(Q_{11}t^2) = \{1/[2(NL)^2]\}(1 - E_2/E_1)(NL - 3) \qquad (17)$$

(where NL is the number of layers) and which appears in Eq. (1) and thereby enables stiffnesses A_{22} and D_{22} to influence the buckling load, also dies out slowly. The maximum coupling occurs for this unsymmetric laminate when $NL = 6$. The magnitudes of, e.g., D_{22} and $B_{11}/(Q_{11}t^2)$ cannot be compared quantitatively. They do not have the same base for normalization (B_{11} cannot be normalized relative to its value for all 0° layers since there its value is zero). Thus, the effect of a single unsymmetrically placed 90° layer on the buckling load is easily seen to die out slowly as the number of layers increases.

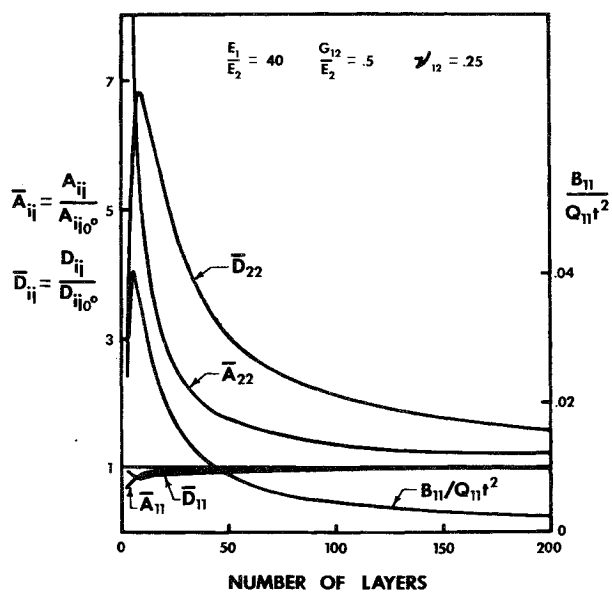

Fig. 12 Normalized stiffnesses of example unsymmetric cross-ply graphite/epoxy laminate.

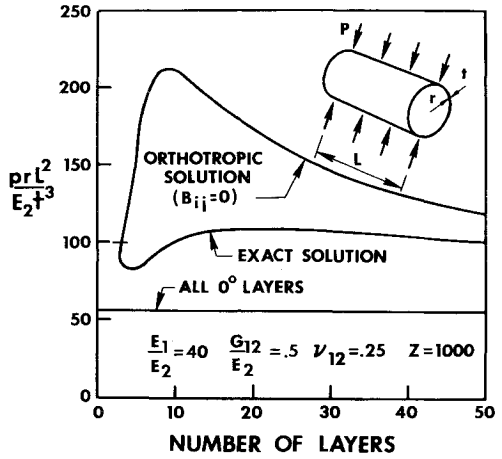

Fig. 13 Normalized lateral pressure buckling loads of unsymmetric cross-ply laminated graphite/epoxy shells.

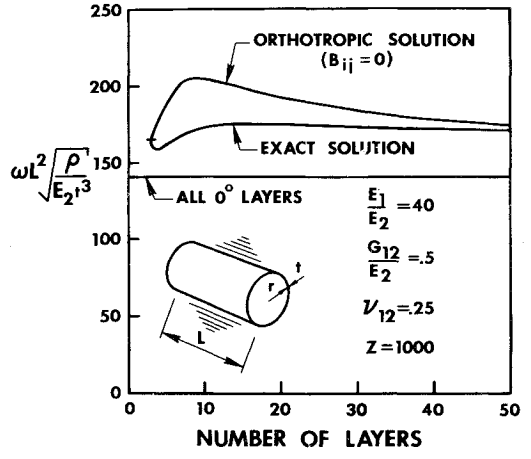

Fig. 14 Normalized fundamental natural frequencies of unsymmetric cross-ply laminated graphite/epoxy shells.

For unsymmetric cross-ply laminates wherein each layer is of the same material but of different orientation (either 0° or 90°, but not necessarily alternating), B_{12} and B_{66} can easily be shown to be zero. Also, B_{11} and B_{22} are not of equal value but opposite sign as for antisymmetric cross-ply laminates. However, for general unsymmetric laminates of different materials, all coupling stiffnesses can occur. The present theory is applicable to the general lamination case as long as the principal material directions of each layer are aligned with the shell coordinate directions.

Lateral Pressure Buckling Results

Normalized lateral pressure buckling loads for unsymmetrically laminated graphite/epoxy shells are shown in Fig. 13 as a function of the number of layers. The shell has all 0° layers except for one 90° layer and a length, radius, and thickness such that $Z = 1000$. The exact, orthotropic, and all 0° layer solutions are identified as was done in the axial compression results. The differences between the exact and orthotropic predictions in Fig. 13 range from 56% less than the orthotropic solution at 6 layers to 38% less at 20 layers to 17% less at 50 layers. In addition, the exact results range from 79% more than the all 0° layer solution at 10 layers to 78% more at 50 layers. These are the largest differences attributed to coupling between bending and extension of unsymmetrically laminated plates and shells observed by the authors.

Vibration Results

Normalized fundamental natural frequencies for the example unsymmetric cross-ply laminated graphite/epoxy shells are shown in Fig. 14. The differences between the results are less than for buckling results because of the square root factor previously mentioned for antisymmetric laminates. The differences between the present exact solution and the alternative design analysis approaches of using an orthotropic solution ($B_{ij} = 0$) or all 0° layers are clearly large enough to warrant consideration in engineering practice.

Summary

Coupling between bending and extension has a large effect on the buckling loads and vibration frequencies of the example unsymmetric cross-ply laminated shells. This conclusion is valid when the laminate has mostly 0° layers with a single 90° layer (for which selected numerical results are given in Table 2). However, when the laminate has mostly 90° layers with a single 0° layer, the present exact results are nearly identical to the orthotropic solution (in which coupling is ignored). Thus, there is an interaction between the lamination sequence and the loading that affects whether coupling is important. Moreover, if the single 90° layer is moved within the laminate as in the 20 layer laminate of Fig. 15, then the amount of coupling between bending and extension varies. Thus, for example, the exact normalized lateral pressure buckling loads for a 20 layer laminate range in Fig. 16 from 41% less than the orthotropic solution when the 90° layer is the first layer to 38% less at the second layer to 26% less at the sixth layer to, of course, the same value when the 90° layer is at the middle of the laminate. Accordingly, even larger effects of coupling between bending and extension than shown in Figs. 11, 13, and 14 are possible. Obviously, smaller effects of coupling can also exist. Therefore, coupling between bending and extension must be included in analysis of all unsymmetric laminates.

Conclusions

Numerical results for buckling and vibration of antisymmetrically and unsymmetrically laminated cross-ply graphite/epoxy and boron/epoxy circular cylindrical shells are presented and discussed. These results are obtained from theories due to Jones[2]

Table 2 Buckling and vibration results for unsymmetric cross-ply laminated graphite/epoxy circular cylindrical shells ($L = 34.64$, $r = 10.0$, $t = 0.12$, $Z = 1000$) $E_1 = 30 \times 10^6$psi, $E_2 = 0.75 \times 10^6$psi, $G_{12} = 0.375 \times 10^6$psi, $\nu_{12} = 0.25$)

Number of layers	N_xL^2/E_2t^3		prL^2/E_2t^3		$\omega L^2(\rho/E_2t^3)^{1/2}$	
	Exact	Orthotropic	Exact	Orthotropic	Exact	Orthotropic
1	1482.0	1482.0	55.90	55.90	142.43	142.43
3	1859.8	1859.8	99.39	99.39	164.66	164.66
10	1987.2	2287.0	100.98	211.09	171.14	204.20
20	2061.8	2133.8	108.00	173.11	174.14	192.74
50	1957.4	1913.2	99.72	119.26	170.69	174.82

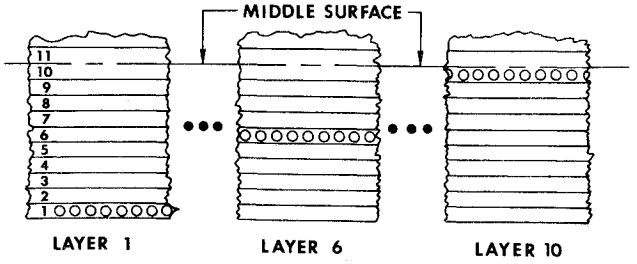

Fig. 15 Position of 90° layer in a 20 layer unsymmetric laminate.

and Dong.[3] There, classical laminated shell theory including the Kirchhoff-Love hypothesis is used for S2 simply supported edge boundary conditions. The shells can be subjected to arbitrary combinations of axial compression and lateral pressure either to cause buckling or to incur a state of initial stress during vibration. For vibration problems, only transverse inertia is considered, i.e., tangential inertia is ignored.

For antisymmetric laminates, buckling results are presented in a generalized Batdorf $k-Z$ form. Coupling between bending and extension leads to buckling loads that are lower than orthotropic predictions by 65% for long graphite/epoxy shells. Conversely, the orthotropic predictions are too high by about 186%. Somewhat smaller differences occur for boron/epoxy shells. Analogous vibration results, with smaller differences than the buckling results, are also presented. For both buckling and vibration of antisymmetric cross-ply shells, the effect of coupling between bending and extension dies out rapidly as the number of layers increases to the point where, for many practical laminates, the effect is unimportant.

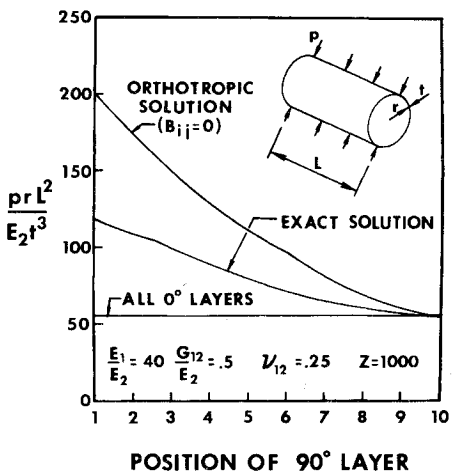

Fig. 16 Effect of 90° layer position on normalized lateral pressure buckling loads of 20 layer unsymmetric cross-ply laminated graphite/epoxy shells.

For unsymmetric laminates, a specific example is used to illustrate what can happen if coupling between bending and extension is ignored. The special example is necessary because general results cannot be presented for a class of laminates with infinite variety. For both buckling and vibration problems, the effect of coupling between bending and extension decreases very *slowly* with an increasing number of layers in contrast to the rapid decrease for antisymmetric laminates. Even for a laminate with as many as *40 layers*, the effect of coupling on the buckling load is about 20% and on the fundamental vibration frequency is about 10%. Another specific laminate example was used to demonstrate that the effect of coupling can be even higher or much lower depending on the distribution of layers in the laminate. Thus, coupling between bending and extension must be accounted for in *all* practical unsymmetric laminates. This conclusion was reached by use of a simple counterexample argument. That is, we found a class of unsymmetric laminates which, even for many layers, exhibits large differences from orthotropic solutions for buckling loads and vibration frequencies because of coupling between bending and extension. Accordingly, the *possibility* of coupling being important for general unsymmetric laminates has been clearly established.

References

[1] Whitney, J. M. and Leissa, A. W., "Analysis of Heterogeneous Anisotropic Plates," *ASME Transactions, Journal of Applied Mechanics*, June 1969, pp. 261–266.

[2] Jones, R. M., "Buckling of Circular Cylindrical Shells with Multiple Orthotropic Layers and Eccentric Stiffeners," *AIAA Journal*, Vol. 6, Dec. 1968, pp. 2301–2305, Errata, Oct. 1969, p. 2048.

[3] Dong, S. B., "Free Vibration of Laminated Orthotropic Cylindrical Shells," *The Journal of the Acoustical Society of America*, Vol. 44, Dec. 1968, pp. 1628–1635.

[4] Almroth, B. O., "Influence of Edge Conditions on the Stability of Axially Compressed Cylindrical Shells," *AIAA Journal*, Vol. 4, Jan. 1966, pp. 134–140.

[5] Cheng, S. and Ho, B. P. C., "Stability of Heterogeneous Aeolotropic Cylindrical Shells Under Combined Loading," *AIAA Journal*, Vol. 1, April 1963, pp. 892–898.

[6] Jones, R. M., "Buckling and Vibration of Unsymmetrically Laminated Cross-Ply Rectangular Plates," *AIAA Journal*, Vol. 11, Dec. 1973, pp. 1626–1632.

[7] Jones, R. M., *Mechanics of Composite Materials*, McGraw-Hill, New York, 1975.

[8] Jones, R. M. and Morgan, H. S., "Buckling and Vibration of Cross-Ply Laminated Circular Cylindrical Shells," AIAA Paper 74-33, Washington D.C., 1974.

[9] Jones, R. M., "Plastic Buckling of Eccentrically Stiffened Multilayered Circular Cylindrical Shells," *AIAA Journal*, Vol. 8, Feb. 1970, pp. 262–270.

[10] Leissa, A. W., *Vibration of Shells*, SP-288, 1973, NASA.

[11] Mikulas, M. M., Jr. and McElman, J. A., *On Free Vibrations of Eccentrically Stiffened Cylindrical Shells and Flat Plates*, TN D-3010, Sept. 1965, NASA.

[12] Card, M. F. and Jones, R. M., *Experimental and Theoretical Results for Buckling of Eccentrically Stiffened Cylinders*, TN D-3639, Oct. 1966, NASA.